Article

J. Biol. Regul. Homeost. Agents. 2025; 39(1): 29–35
https://doi.org/10.23812/j.biol.regul.homeost.agents.20253901.4

HO-1 Prevents Oxidative Stress Damage, Promotes Proliferation and Inhibits Apoptosis of Osteoblasts Induced by H_2O_2

Maimaiti Xiayimaierdan[1], Jinyong Huang[2], Chenchen Fan[1], Feiyu Cai[1], Zengru Xie[2,*]

[1]Departments of Microrepair and Reconstruction, The First Affiliated Hospital of Xinjiang Medical University, 830054 Urumqi, Xinjiang Uygur Autonomous Region, China
[2]Traumatic Surgery, The First Affiliated Hospital of Xinjiang Medical University, 830054 Urumqi, Xinjiang Uygur Autonomous Region, China
*Correspondence: xiezengrru@163.com (Zengru Xie)
Submitted: 24 August 2022 Revised: 29 November 2022 Accepted: 16 December 2022 Published: 16 January 2025

Background: Hydrogen peroxide (H_2O_2) can induce oxidative injury, protein damage and DNA breaks in osteoblasts. The purpose of this study was to investigate the effect of heme oxygenase-1 (HO-1) on the biological behavior and oxidative stress damage of H_2O_2-treated osteoblasts.

Methods: The skull osteoblasts were isolated and divided into three groups: negative control group (without H_2O_2 or transfection of HO-1 protein), positive control group (with H_2O_2 but without transfection of HO-1 protein) and experimental group (with H_2O_2 and transfection of HO-1 protein). After 24 h of intervention, the apoptosis, cell proliferation, levels of reactive oxygen species (ROS), malondialdehyde (MDA) and superoxide dismutase (SOD), protein levels of B-cell lymphoma-2 (Bcl-2), Caspase-3, Tartrate resistant acid phosphatase (TRAP) and cytokinin (CTK), as well as protein and mRNA levels of bone gla-protein (BGP) and Runt related transcription factor 2 (Runx2) were detected.

Results: Compared with the negative control group, the positive control group and the experimental group had lower levels of SOD, lower protein and mRNA expressions of BGP and Runx2, higher cell proliferation inhibition rate, apoptosis rate, levels of MDA and ROS levels, and protein levels of Bcl-2, Caspase-3, TRAP and CTK after intervention (all $p < 0.05$). The experimental group showed the opposite results when comparing with the positive control group (all $p < 0.05$).

Conclusions: HO-1 can inhibit the oxidative stress damage of osteoblasts induced by H_2O_2, as well as promote the proliferation and inhibit the apoptosis of osteoblasts.

Keywords: heme oxygenase-1; osteoblasts; apoptosis; proliferation; oxidative stress

Introduction

Osteoporosis is a systemic metabolic disease characterized by abnormal bone tissue structure and decreased bone mass, which is an independent risk factor for fractures. The incidence of osteoporosis in people over 50 years old in China is over 18.6%. The risk of fractures increases if osteoporosis is not treated in time which threatening the health and quality of life of patients [1–3]. Therefore, exploring the possible mechanism of osteoporosis is of important clinical significance for the prevention and treatment of fractures.

Oxidative stress refers to the process in which insufficient removal of reactive oxygen species (ROS) leads to oxidative damage on tissues [4,5]. Study has confirmed that oxidative stress is closely related to the occurrence of osteoporosis [6]. When the body is in a state of oxidative stress, the activity of Wnt and other signaling pathways will be activated, which inhibits the proliferation of osteoblasts and increases the activity of osteoclasts, leading to the breakdown of the dynamic balance between osteoblasts and osteoclasts and eventually the increasing risk of osteoporosis [7]. Therefore, regulation of oxidative stress state is currently one of the clinical treatments for osteoporosis. Notably, oxidative stress model is often constructed using hydrogen peroxide (H_2O_2) because it is the most abundant superoxide dismutase (SOD) in living cells and its accumulation leads to oxidative stress [8,9]. So, $H_2O_2$was chose to stimulate oxidative stress damage in osteoblasts in this study. As a member of heme oxygenase, heme oxygenase 1 (HO-1) has strong anti-inflammatory and antioxidant functions [10]. HO-1 is activated by stimulation of inflammatory factors or the state of oxidative stress [11]. HO-1 plays an important role in osteocyte homeostasis [12]. Most studies explored the expression of HO-1 in osteoblasts damaged by oxidative stress, but there are few reports about HO-1 regulating biological behavior of osteoblasts. Therefore, this study aimed to provide novel ideas for the treatment of osteoporosis by exploring the effects of HO-1 on the biological behavior and oxidative stress damage of osteoblasts induced by H_2O_2.

Journal of
BIOLOGICAL REGULATORS
and Homeostatic Agents

Table 1. Primer sequences used in this study.

Primer	Sequence
BGP forward primer	5′-GGACCATCTTTCTGCTCACTCTG-3′
BGP reverse primer	5′-GTTCACTACCTTATTGCCCTCCTG-3′
Runx2 forward primer	5′-TTATTCTGCTGAGCTCCGG-3′
Runx2 reverse primer	5′-GTGAAACTCTTGCCTCGTC-3′
GADPH forward primer	5′-GAAGGTGAAGGTCGGAGTC-3′
GADPH reverse primer	5′-GAAGATGGTGATGGGATTTC-3′

Materials and Methods

Animals

Specific-pathogen-free (SPF)-grade male Sprague-Dawley (SD) suckling mice born within 24 h, regardless of sex were adaptively housed in a barrier environment at 21 °C and 50% of humidity for 1 week (certificate No.SCXK 2019-0048). This study was approved by the Animal Ethics Committee of Sichuan Laboratory Animal Center, China (No.2019-0324).

Main Experimental Reagents and Instruments Reagents

The manufacturers of the reagents were as follows: HO-1 eukaryotic expression plasmid (Genview, USA), H_2O_2 (Sigma, US), 3-(4,5)-dimethylthiahiazo (-z-y1)-3,5-di- phenytetrazoliumromide (MTT) kit (Genview, USA), Lipofectamine 3000 transfection kit (Merck, Germany), Takara two-step reverse transcription-polymerase chain reaction (RT-PCR) kit (Takara, Japan), SYBR RT-PCR kit (Hangzhou Bori Technology, China), apoptosis detection kit (Genview, USA), ROS fluorescent probe kit (Beijing Dingguo Biotechnology, China), malondialdehyde (MDA; Cat. 9890) and superoxide dismutase (SOD; Cat. 9266) kits (Beijing Dingguo Biotechnology, China), Bcl-2 (ab182858, Abcam, UK) Caspase-3 (ab32351, Abcam, UK), Tartrate resistant acid phosphatase (TRAP; ab133238, Abcam, UK), cytokinin (CTK; ab47812, Abcam, UK), bone gla-protein (BGP; ab108397, Abcam, UK), Runt related transcription factor 2 (Runx2) mouse polyclonal antibody (ab192256, Abcam, UK), mouse anti-β-actin (ab8226, Abcam, UK), HRP labeled goat anti-mouse secondary antibody (ab6721, Abcam, UK), ECL high-efficiency chemiluminescence kits (Genview, US). BGP, Runx2 and GADPH primers were designed and synthesized by Beijing Dingguo Biotechnology, China. The primer sequences are shown in Table 1.

The manufacturers of the instruments are as follows: Optical microscope (BX53, Olympus, Japan), real-time PCR instrument (MX3000P, GENE, USA), microplate reader (450, Bio Rad, USA), JY-SCZ2 SDS-PAGE protein electrophoresis instrument (Beijing Liuyi Instrument, China), FACS flow cytometer (Becton, Dickinson and Company, USA), Transwell chamber (Corning Costar Corp, USA) and iX71 fluorescence microscope (Olympus, Tokyo, Japan).

Cell Culture

After the suckling mice were sacrificed by cervical dislocation, they were immediately immersed in 75% alcohol for 5 min. Thereafter, the skull was extracted in a sterile environment, placed in a Dulbecco's modified eagle medium (DMEM; GIBICO, MA, USA) removed for the residue and adipose tissues and cut into small pieces. The medium was added with an appropriate amount of 0.25% trypsin and type I collagenase. After pipetting and mixing, the sample was placed at room temperature for 10 min, then centrifuged at 1500 r/min for 5 min, removed for the supernatant and added with complete medium. Again, after pipetting and mixing, the sample was placed at 37 °C and cultivated in 5% CO_2. The purity was identified by Von Kossa staining. The osteoblasts were visible under the microscope as black particles after staining [13]. The culture medium was replaced once every 24 h. Subculture was conducted when the fraction of coverage of cells reached 80%. Logarithmic growth phase cells were used for subsequent experiments.

Grouping

Logarithmic osteoblasts were inoculated in 6-well or 96-well plates and divided into 3 groups: negative control group, positive control group and experimental group. The experimental group was added with 100 μmol/L H_2O_2 and transfected with HO-1 protein plasmid according to Lipofectamine 3000 Transfection kit. The positive control group was added with 100 μmol/L H_2O_2, and the negative control group was added with the same amount of dimethyl sulfoxide (DMSO). The culture medium was discarded after 24 h of intervention, and new DMEM was added for subsequent experiments in all groups.

MTT Assay

The osteoblasts at logarithmic growth phase were inoculated in a 96-well plate at a concentration of 2.5×10^5/mL (199 μL per well) and cultured in an incubator for 24 h. Then the cells were intervened (see grouping method above). The MTT assay was performed after 24 h of intervention, and the optical density (OD) of each well was measured with an enzyme-linked immunoassay at 490 nm. The inhibition rate of cell proliferation = 1 – (OD value of intervened group – OD value of zero set group)/(OD value of the control group – OD value of zero set group) × 100%, repeating 3 times.

Detection of Apoptosis

The osteoblasts at logarithmic phase were seeded in a 6-well plate (see grouping method above). After 24 h of intervention, the cells were collected by trypsin digestion, washed with phosphate buffered saline (PBS) and detected for the apoptosis rate by Flow cytometry. The operations were carried out strictly in accordance with the instruction

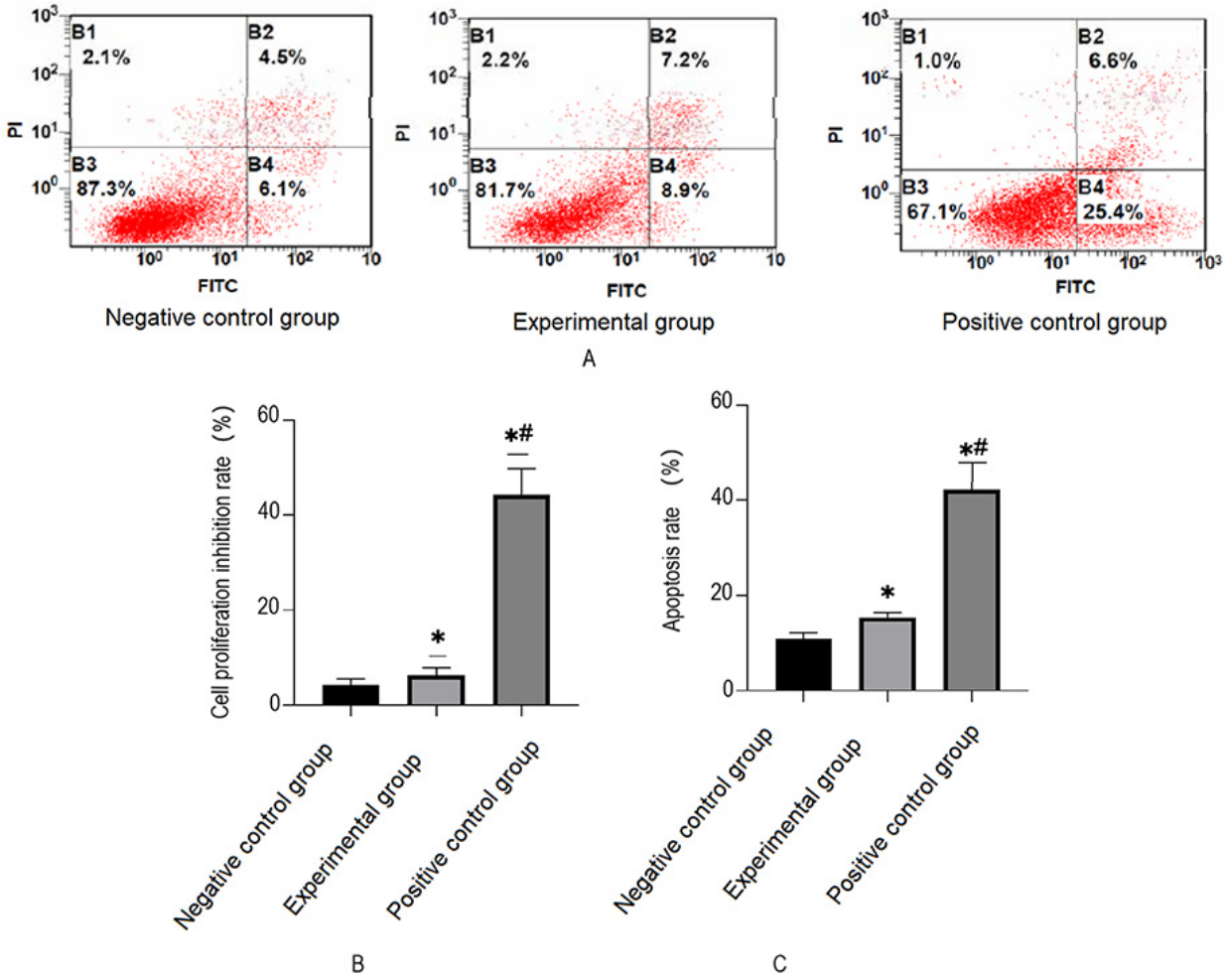

Fig. 1. Comparison of cell proliferation inhibition rate and cell apoptosis rate among the three groups. (A) Flow cytometric apoptosis diagram. (B) Cell proliferation inhibition rates (%). (C) Cell apoptosis rate (%). Compared with the negative control group, $^{*}p < 0.05$; compared with the experimental group, $^{\#}p < 0.05$.

of apoptosis kit. The laser wavelength was 488 nm, and the emitted wavelength was greater than 630 nm. Annexin V-stained cells were in the early-apoptotic stage. PI-stained cells were dead cells. Double-stained cells were in the mid-apoptotic stage.

Detection of ROS

The osteoblasts at logarithmic phase were seeded in a 6-well plate (see grouping method above). After 24 h of intervention, the culture plate was washed and stained with working solution (DCFA-DA:D-hanks = 1:1000) at 37 °C for 30 min. Then the cells were washed and observed under a fluorescence microscope at a wavelength of 490 mm. Image J software (Image J 1.5, NIH, USA) was used to analyze the fluorescence signal.

Detection of MDA and SOD

The osteoblasts at logarithmic phase were seeded in a 6-well plate (see grouping method above). After 24 h of intervention, the cells were washed, lysed and centrifuged at 3000 r/min for 5 min. The supernatant was taken to detect the contents of MDA and SOD by corresponding kits according to the instructions.

qRT-PCR

The osteoblasts at logarithmic phase were seeded in a 6-well plate (see grouping method above). The cells were collected after 24 h of intervention. RNA extraction kit was used to extract cRNA, and qRT-PCR experiments were performed according to the instructions of SYBR RT-PCR kit after reverse transcription, reaction condition included: predenaturation at 95 °C for 30 s, then 35 cycles of denaturation at 95 °C for 5 s and annealing at 60 °C for 30 s. The $2^{-\Delta\Delta Ct}$ method [14] was used to determine the relative mRNA expression of BGP and Runx2 in each group, with GADPH as an internal reference. Each sample was detected for 3 times, and the average value was calculated.

Journal of
BIOLOGICAL REGULATORS
and Homeostatic Agents

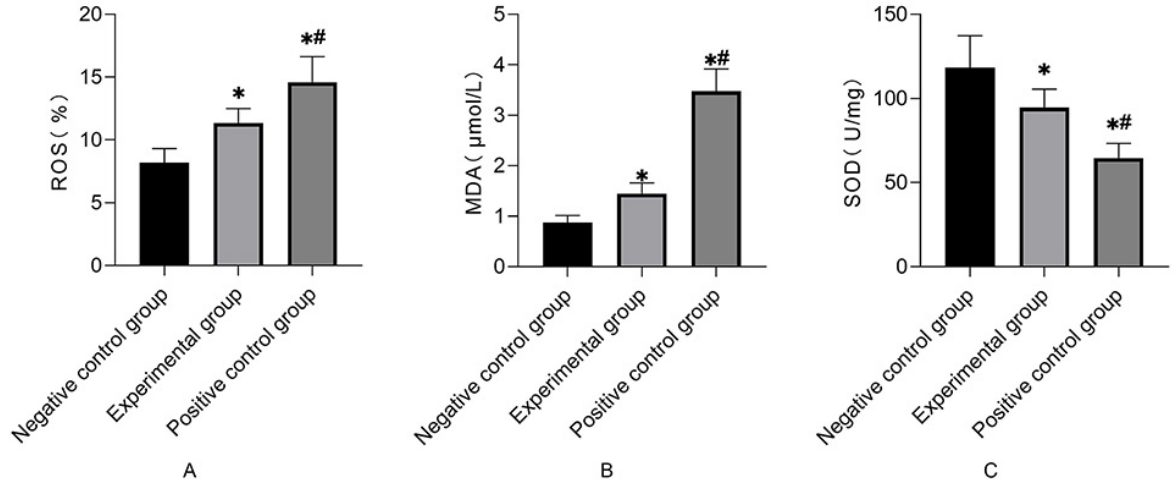

Fig. 2. Comparative analysis of the levels of ROS, MDA and SOD in osteoblasts. (A) Comparison of ROS levels among the three groups. (B) Comparison of MDA levels among the three groups. (C) Comparison of SOD levels among the three groups. Compared with the negative control group, $^{*}p < 0.05$; compared with the experimental group, $^{\#}p < 0.05$. ROS, Reactive oxygen species; MDA, Malondialdehyde; SOD, Superoxide dismutase.

Western Blot

The osteoblasts at logarithmic phase were seeded in a 6-well plate (see grouping method above). The cells were collected after 24 h of intervention, extracted for the total protein via protein extraction kit and determined for the concentration of Bcl-2, BGP, Runx2, TRAP and CTK. The sample was given electrophoresis, transferred and blocked according to the instructions of the Western blot kit. Then, the sample was added with diluted mouse antibodies (Bcl-2 dilution ratio: 1:300; Caspase-3 dilution ratio: 1:500; TRAP dilution ratio: 1:300; CTK dilution ratio: 1:300; BGP dilution ratio: 1:800; Runx2 dilution ratio: 1:500; β-actin dilution ratio: 1:1000) and incubated overnight. The next day, the sample was washed with TBST, added with HRP-labeled goat anti-mouse secondary antibody (dilution ratio 1:500), incubated for 2 h and exposed in a dark room for imaging. The image bands were analyzed for the gray value by ImageJ software (Image J 1.5, NIH, USA) and calculated for the relative protein expression, repeating 3 times.

Statistical Analysis

Statistical analysis was performed using Statistical Product Service Solutions (SPSS) version 22.0 (International Business Machines, corp., Armonk, NY, USA). Measurement data were expressed as means ± standard deviation (SD). The differences among groups were compared using one-way analysis of variance (ANVOA). Pairwise comparison between groups was performed by Student-Newman-Keuls test. The difference was statistically significant when $p < 0.05$.

Results

Effects of HO-1 on Cell Proliferation and Apoptosis in H_2O_2-Treated Osteoblasts

Cell proliferation and apoptosis were compared among the three groups (Fig. 1A–C). Compared with the negative control group, the cell proliferation inhibition rate (Fig. 1B) and apoptosis rate (Fig. 1C) increased in the experimental group treated with HO-1 and H_2O_2 and the positive control group treated with H_2O_2 (all $p < 0.05$). The two rates were higher in the positive control group than those in the experimental group (both $p < 0.05$). It was indicated that HO-1 inhibited H_2O_2-induced cell proliferation inhibition and apoptosis of osteoblasts.

Effects of HO-1 on the Contents of ROS, MDA and SOD in H_2O_2-Treated Osteoblasts

To evaluate the influence of HO-1 on H_2O_2-induced oxidative stress in osteoblasts, the levels of ROS (Fig. 2A), MDA (Fig. 2B) and SOD (Fig. 2C) among the three groups were shown in Fig. 2. Compared with the negative control group, the SOD levels were lower, while the MDA and ROS levels were increased in the positive control group and experimental group (all $p < 0.05$). The positive control group had a decreased level of SOD as well as increased levels of MDA and ROS as compared to the experimental group (all $p < 0.05$), suggesting that HO-1 decreased H_2O_2-induced ROS and MDA levels and increased H_2O_2-inhibited SOD levels of osteoblasts. Above results proved that HO-1 inhibited H_2O_2-induced oxidative stress in osteoblasts.

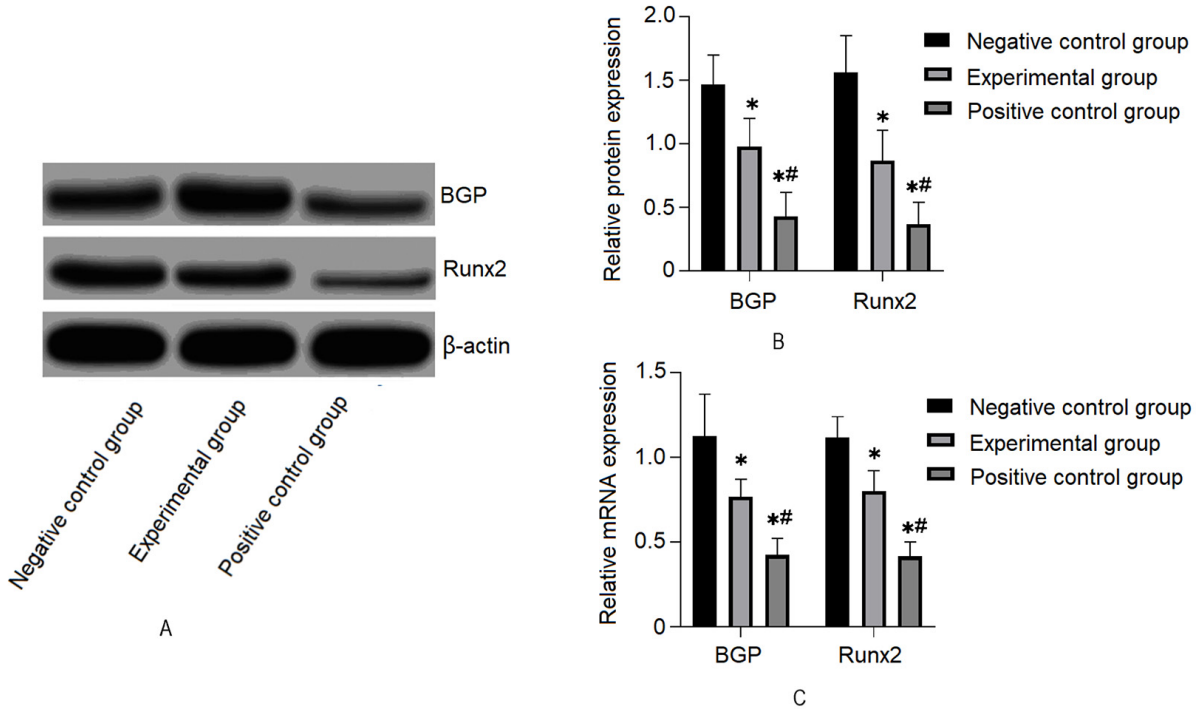

Fig. 3. Comparative analysis of protein levels of BGP and Runx2 in osteoblasts. (A) A representative immunoblotting image with BGP and Runx2 protein bands from osteoblasts. (B) Comparative analysis of relative protein expression levels of BGP and Runx2 among the groups. Compared with the negative control group, $^{*}p < 0.05$; compared with the experimental group, $^{\#}p < 0.05$. BGP, Bone gla-protein; Runx2, Runt Related Transcription Factor 2.

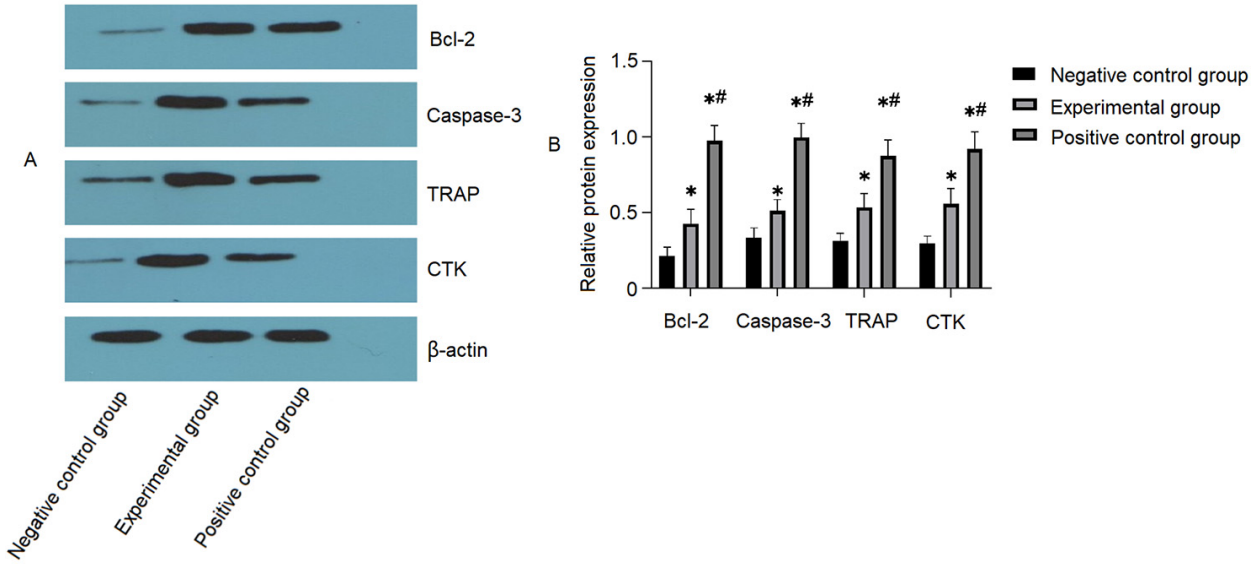

Fig. 4. Comparative analysis of protein levels of Bcl-2, Caspase-3, TRAP and CTK in osteoblasts. (A) A representative immunoblotting image with the bands of protein of interest. (B) Comparative analysis of protein expression levels. Compared with the negative control group, $^{*}p < 0.05$; compared with the experimental group, $^{\#}p < 0.05$. Bcl-2, B-cell lymphoma-2; TRAP, Tartrate resistant acid phosphatase; CTK, Cytokinin.

Effects of HO-1 on Protein and mRNA Levels of BGP and Runx2 in H_2O_2-Treated Osteoblasts

The protein (Fig. 3A,B) and mRNA (Fig. 3C) levels of BGP and Runx2 among the three groups were shown in Fig. 3. Compared with the negative control group, the protein and mRNA levels of BGP and Runx2 were decreased in the positive control group and the experimental group (all $p < 0.05$). Compared to the positive control group, protein

Journal of
BIOLOGICAL REGULATORS
and Homeostatic Agents

and mRNA levels of BGP and Runx2 was increased in the experimental group ($p < 0.05$), indicating that HO-1 upregulated BGP and Runx2 expression levels in H_2O_2-treated osteoblasts.

Effects of HO-1 on Protein Levels of Bcl-2, Caspase-3, TRAP and CTK in H_2O_2-Treated Osteoblasts

Protein levels of Bcl-2, Caspase-3, TRAP and CTK were demonstrated among the three groups, as shown in Fig. 4A. Compared with the negative control group, the positive control group and the experimental group have higher relative levels of Bcl-2, Caspase-3, TRAP, and CTK proteins (Fig. 4B; all $p < 0.05$). Compared with the positive control group, an increase in the relative levels of Bcl-2, Caspase-3, TRAP and CTK proteins was demonstrated in the experimental group (Fig. 4B; all $p < 0.05$), indicating that HO-1 downregulated Bcl-2, Caspase-3, TRAP, and CTK protein expression levels in H_2O_2-treated osteoblasts.

Discussion

Oxidative stress plays an important role in the biological activity of osteoblasts [15–19]. HO-1 is the rate-limiting enzyme of heme decomposition which can be activated by cytokines and oxidative stress factors. HO-1 shows effect on anti-inflammation and anti-oxidative stress and is considered as a body protective protein. It is found that HO-1 is closely related to cell apoptosis in body and has a regulatory effect on the apoptosis pathway [20]. In addition, HO-1 can inhibit the differentiation of bone marrow mesenchymal stem cells into adipocytes, thereby promoting their differentiation into osteoblasts, so as to facilitate the proliferation of osteoblasts and enhance the mineralization ability of cells [21]. Another study showed a reduced expression level of HO-1 in patients with osteoporosis [13]. Therefore, we established an oxidative stress injury model of osteoblasts to explore the effects of HO-1 on osteoblasts. The results of MTT and apoptosis experiments showed that after HO-1 transfection, the cell proliferation inhibition rate and the apoptosis rate are reduced as compared with those of the oxidative stress injury model of osteoblasts. In addition, compared with normal osteoblasts, the expression level of apoptosis-related proteins, Bcl-2 and Caspase-3 are overexpressed in the oxidative stress injury model of osteoblasts. After transfection with HO-1, the levels of apoptosis-related proteins, Bcl-2 and Caspase-3 decrease. It is suggested that HO-1 can promote the proliferation and inhibit the apoptosis in H_2O_2-treated osteoblasts.

High level of ROS can promote the expression of inflammatory factors, which in turn activates the molecular cascade and promotes the expression of apoptosis-related proteins, Bcl-2 and Caspase-3, etc. [22]. The results of this study showed that compared with normal osteoblasts, the level of ROS increases significantly in the oxidative stress injury model of osteoblasts. After transfection with HO-1, the levels of cellular ROS decreases. SOD has an effect of anti-inflammation and scavenging of free radicals, and excessive MDA level indicates cell damage, both of which play an important role in the process of cell oxidative stress damage [23,24]. This study found that the level of MDA increases while the level of SOD decreases significantly in the oxidative stress injury model of osteoblasts. After HO-1 transfection, the SOD level increases, while the MDA level decreases. The above results all suggested that after HO-1 transfection, the oxidative stress damage is controlled to a certain extent.

As osteoblast differentiation markers, BGP and Runx2 act as an important role in the proliferation and differentiation of osteoblasts [25,26]. TRAP, which highly expressed in osteoclasts, is one of osteoclast-specific markers [27]. CTK is an osteoclast collagen lytic enzyme and plays an important role in osteoclast bone resorption [28]. The results of this study showed that after HO-1 transfection, the protein and mRNA levels of Runx2 and BGP increase significantly, while the protein levels of TRAP and CTK decrease compared to the oxidative stress injury model of osteoblasts. From a molecular point of view, this study also proved that HO-1 transfection can promote the differentiation of osteoblasts and inhibit the expression of osteoclast-related proteins.

However, this study also has some limitations. First, we did not conduct *in vivo* experiments to verify whether HO-1 up-regulation can inhibit oxidative stress damage of osteoblasts at the level of the organism. Second, we did not explore the changes of the related indicators at different time points to obtain the dynamics data. Therefore, it is still necessary to carry out a further study on this topic.

Conclusions

In summary, HO-1 can inhibit oxidative stress damage of osteoblasts induced by H_2O_2, as well as promote proliferation and inhibit apoptosis of osteoblasts, which provides some basic data for follow-up discussion on the treatment or prevention of osteoporosis.

Ethics Approval and Consent to Participate

This study was approved by the Animal Ethics Committee of Sichuan Laboratory Animal Center, China (No.2019-0324).

Funding

This work was supported by the Natural Science Foundation of Xinjiang Uygur Autonomous Region (No. 2020D01C264).

Conflict of Interest

The authors declare no conflict of interest.

References

[1] Jabran A, Peach C, Ren L. Biomechanical analysis of plate systems for proximal humerus fractures: a systematic literature review. Biomedical Engineering Online. 2018; 17: 47.

[2] Chen H, Yin P, Wang S, Li J, Zhang L, Khan K, *et al*. The Augment of the Stability in Locking Compression Plate with Intramedullary Fibular Allograft for Proximal Humerus Fractures in Elderly People. BioMed Research International. 2018; 2018: 3130625.

[3] Plath JE, Kerschbaum C, Seebauer T, Holz R, Henderson DJH, Förch S, *et al*. Locking nail versus locking plate for proximal humeral fracture fixation in an elderly population: a prospective randomised controlled trial. BMC Musculoskeletal Disorders. 2019; 20: 20.

[4] Guzik TJ, Touyz RM. Oxidative Stress, Inflammation, and Vascular Aging in Hypertension. Hypertension. 2017; 70: 660–667.

[5] Yao H, Yao Z, Zhang S, Zhang W, Zhou W. Upregulation of SIRT1 inhibits H2O2 induced osteoblast apoptosis via FoxO1/β catenin pathway. Molecular Medicine Reports. 2018; 17: 6681–6690.

[6] Li DY, Yu JC, Xiao L, Miao W, Ji K, Wang SC, *et al*. Autophagy attenuates the oxidative stress-induced apoptosis of Mc3T3-E1 osteoblasts. European Review for Medical and Pharmacological Sciences. 2017; 21: 5548–5556.

[7] De-Ugarte L, Balcells S, Nogues X, Grinberg D, Diez-Perez A, Garcia-Giralt N. Pro-osteoporotic miR-320a impairs osteoblast function and induces oxidative stress. PLoS ONE. 2018; 13: e0208131.

[8] Li X, Chen Y, Mao Y, Dai P, Sun X, Zhang X, *et al*. Curcumin Protects Osteoblasts From Oxidative Stress-Induced Dysfunction via GSK3β-Nrf2 Signaling Pathway. Frontiers in Bioengineering and Biotechnology. 2020; 8: 625.

[9] Yoon JY, Kim DW, Kim EJ, Park BS, Yoon JU, Kim HJ, *et al*. Protective effects of remifentanil against H_2O_2-induced oxidative stress in human osteoblasts. Journal of Dental Anesthesia and Pain Medicine. 2016; 16: 263–271.

[10] Zhang D, Xiao Y, Lv P, Teng Z, Dong Y, Qi Q, *et al*. Edaravone attenuates oxidative stress induced by chronic cerebral hypoperfusion injury: role of ERK/Nrf2/HO-1 signaling pathway. Neurological Research. 2018; 40: 1–10.

[11] Zeng X, Feng Q, Zhao F, Sun C, Zhou T, Yang J, *et al*. Puerarin inhibits TRPM3/miR-204 to promote MC3T3-E1 cells proliferation, differentiation and mineralization. Phytotherapy Research. 2018; 32: 996–1003.

[12] Xiu D, Wang Z, Cui L, Jiang J, Yang H, Liu G. Sumoylation of SMAD 4 ameliorates the oxidative stress-induced apoptosis in osteoblasts. Cytokine. 2018; 102: 173–180.

[13] Wang R, Shen Z, Yang L, Yin M, Zheng W, Wu B, *et al*. Protective effects of heme oxygenase-1-transduced bone marrow-derived mesenchymal stem cells on reduced size liver transplantation: Role of autophagy regulated by the ERK/mTOR signaling pathway. International Journal of Molecular Medicine. 2017; 40: 1537–1548.

[14] Livak KJ, Schmittgen TD. Analysis of relative gene expression data using real-time quantitative PCR and the 2(-Delta Delta C(T)) Method. Methods. 2001; 25: 402–408.

[15] Lee WC, Guntur AR, Long F, Rosen CJ. Energy Metabolism of the Osteoblast: Implications for Osteoporosis. Endocrine Reviews. 2017; 38: 255–266.

[16] He XF, Zhang L, Zhang CH, Zhao CR, Li H, Zhang LF, *et al*. Berberine alleviates oxidative stress in rats with osteoporosis through receptor activator of NF-kB/receptor activator of NF-kB ligand/osteoprotegerin (RANK/RANKL/OPG) pathway. Bosnian Journal of Basic Medical Sciences. 2017; 17: 295–301.

[17] Bonaccorsi G, Piva I, Greco P, Cervellati C. Oxidative stress as a possible pathogenic cofactor of post-menopausal osteoporosis: Existing evidence in support of the axis oestrogen deficiency-redox imbalance-bone loss. The Indian Journal of Medical Research. 2018; 147: 341–351.

[18] Ghorabi MT, Aliaghaei A, Sadeghi Y, Shaerzadeh F, Rad AA, Mohamadi R, *et al*. Evidence supporting neuroprotective effect of adipose derived stem cells on PC12 cells against oxidative stress induced by H2O2. Cellular and Molecular Biology. 2017; 63: 1–6.

[19] Prior JC, Seifert-Klauss VR, Giustini D, Adachi JD, Kalyan S, Goshtasebi A. Estrogen-progestin therapy causes a greater increase in spinal bone mineral density than estrogen therapy - a systematic review and meta-analysis of controlled trials with direct randomization. Journal of Musculoskeletal & Neuronal Interactions. 2017; 17: 146–154.

[20] Araujo JA, Zhang M, Yin F. Heme oxygenase-1, oxidation, inflammation, and atherosclerosis. Frontiers in Pharmacology. 2012; 3: 119.

[21] Cremers NAJ, Lundvig DMS, van Dalen SCM, Schelbergen RF, van Lent PLEM, Szarek WA, *et al*. Curcumin-induced heme oxygenase-1 expression prevents H2O2-induced cell death in wild type and heme oxygenase-2 knockout adipose-derived mesenchymal stem cells. International Journal of Molecular Sciences. 2014; 15: 17974–17999.

[22] Zhou H, Yang J, Xin T, Li D, Guo J, Hu S, *et al*. Exendin-4 protects adipose-derived mesenchymal stem cells from apoptosis induced by hydrogen peroxide through the PI3K/Akt-Sfrp2 pathways. Free Radical Biology & Medicine. 2014; 77: 363–375.

[23] Shakeri F, Boskabady MH. Anti-inflammatory, antioxidant, and immunomodulatory effects of curcumin in ovalbumin-sensitized rat. BioFactors. 2017; 43: 567–576.

[24] Tsikas D. Assessment of lipid peroxidation by measuring malondialdehyde (MDA) and relatives in biological samples: Analytical and biological challenges. Analytical Biochemistry. 2017; 524: 13–30.

[25] Komori T. Signaling networks in RUNX2-dependent bone development. Journal of Cellular Biochemistry. 2011; 112: 750–755.

[26] Xiao G, Jiang D, Ge C, Zhao Z, Lai Y, Boules H, *et al*. Cooperative interactions between activating transcription factor 4 and Runx2/Cbfa1 stimulate osteoblast-specific osteocalcin gene expression. The Journal of Biological Chemistry. 2005; 280: 30689–30696.

[27] Kirstein B, Chambers TJ, Fuller K. Secretion of tartrate-resistant acid phosphatase by osteoclasts correlates with resorptive behavior. Journal of Cellular Biochemistry. 2006; 98: 1085–1094.

[28] Linsuwanont B, Takagi Y, Ohya K, Shimokawa H. Localization of cathepsin K in bovine odontoclasts during deciduous tooth resorption. Calcified Tissue International. 2002; 70: 127–133.